Blood vessel endothelial VEGFR-2 delays lymphangiogenesis: an endogenous trapping mechanism links lymph- and angiogenesis

Shintaro Nakao,[1,2] *Souska Zandi,[1] *Yasuaki Hata,[2] Shuhei Kawahara,[2] Ryoichi Arita,[2] Alexander Schering,[1] Dawei Sun,[1] Mark I. Melhorn,[1] Yasuhiro Ito,[1] Nuria Lara-Castillo,[1] Tatsuro Ishibashi,[2] and Ali Hafezi-Moghadam[1]

[1]Angiogenesis Laboratory, Massachusetts Eye and Ear Infirmary, Department of Ophthalmology, Harvard Medical School, Boston, MA; and [2]Department of Ophthalmology, Graduate School of Medical Sciences, Kyushu University, Fukuoka, Japan

Angio- and lymphangiogenesis are inherently related processes. However, how blood and lymphatic vessels regulate each other is unknown. This work introduces a novel mechanism explaining the temporal and spatial relation of blood and lymphatic vessels. Vascular endothelial growth factor-A (VEGF-A) surprisingly reduced VEGF-C in the supernatant of blood vessel endothelial cells, suggesting growth factor (GF) clearance by the growing endothelium. The orientation of lymphatic sprouting toward angiogenic vessels and away from exogenous GFs was VEGF-C dependent. In vivo molecular imaging revealed higher VEGF receptor (R)-2 in angiogenic tips compared with normal vessels. Consistently, lymphatic growth was impeded in the angiogenic front. VEGF-C/R-2 complex in the cytoplasm of VEGF-A–treated endothelium indicated that receptor-mediated internalization causes GF clearance from the extracellular matrix. GF clearance by receptor-mediated internalization is a new paradigm explaining various characteristics of lymphatics. (*Blood*. 2011; 117(3):1081-1090)

Introduction

Lymphatic vessels critically contribute to tissue fluid homeostasis and immunity in health and disease.[1] Lymphatic drainage is of eminent clinical relevance, as it facilitates movement of immune or cancer cells throughout the body. Lymphangiogenesis, the growth of new lymphatic vessels, is intensively studied, and there is considerable interest in elucidating the factors that cause it.[1]

Various growth factors (GFs) cause both angio- and lymphangiogenesis, albeit some preferentially bind to receptors on lymphatic and others on blood vessel endothelium.[2] Except for certain circumstances, selective lymphangiogenesis does not occur in vivo.[3-6] This has led to the assumption that angiogenic vascular guidance is a prerequisite for lymphangiogenesis, albeit the details of how angiogenesis might regulate lymphangiogenesis are not understood. Furthermore, it is unknown whether blood and lymphatic vessels interact with or influence each other under pathological conditions.[7]

Vascular endothelial growth factor-C (VEGF-C) and VEGF-D are the only known ligands for VEGF receptor-3 (VEGFR-3) and do not bind to VEGFR-1.[8,9] Proteolytically processed VEGF-C binds to and activates VEGFR-2, while the unprocessed precursor form of VEGF-C signals through VEGFR-3.[10] Both VEGF-C and VEGF-D primarily affect development of lymphatic vasculature through VEGFR-3 activation, but they also participate in angiogenesis through VEGFR-2.[11] For instance, a soluble VEGFR-2 form that is secreted by corneal epithelial cells selectively suppresses the physiologic growth of lymphatics; however, it does not address the interdependency of lymph- and angiogenesis.[5] VEGF-C expression is higher in blood vessel endothelium than in lymphatic endothelium; conversely, VEGFR-3 expression is higher in lymphatic endothelium.[2,12] In comparison, VEGFR-2 expression is similar in both endothelial cell types.[2] However, the differential contribution of VEGF-C/VEGFR-2 interaction to lymph- and angiogenesis is not understood.

VEGF-A is up-regulated in various physiological and pathological conditions, causing endothelial permeability,[13] lymph-,[14-16] and angiogenesis.[17] VEGF-A induces proliferation and migration of the lymphatic endothelium through the VEGFR-2.[12,16,18] However, whether different doses of VEGF-A preferentially cause lymph- or angiogenesis is unknown.

Lymphangiogenesis and angiogenesis occur in concert.[19] However, the molecular mechanisms underlying their temporal and spatial interdependencies are not understood. This work addresses the molecular links between these 2 related processes.

Methods

Animals

All animal experiments were approved by the Animal Care Committee of the Massachusetts Eye and Ear Infirmary. Male 6- to 12-week-old C57BL/6J mice were purchased from The Jackson Laboratory.

Corneal micropocket assay in mice

C57BL/6J mice were anesthetized with an intraperitoneal injection of ketamine (100 mg/kg) and xylazine (10 mg/kg). Hydron pellets (0.3 μL) containing 25, 100, 200, 400, or 1600 ng human (h)VEGF-A (293-VE; R&D Systems), 200 ng mouse VEGF-A (493-MV; R&D Systems), or 400 ng VEGF-C (2176-VC; R&D Systems) were prepared and implanted into the corneas. Pellets were positioned in around 1.0 ± 0.2 mm distance to the corneal limbus. After implantation, bacitracin ophthalmic ointment (E. Fougera & Co.) was applied to each eye to prevent an infection. On the

Submitted February 2, 2010; accepted June 29, 2010. Prepublished online as *Blood* First Edition paper, August 12, 2010; DOI 10.1182/blood-2010-02-267427.

*S.Z. and Y.H. contributed equally to this work.

The online version of this article contains a data supplement.

The publication costs of this article were defrayed in part by page charge payment. Therefore, and solely to indicate this fact, this article is hereby marked "advertisement" in accordance with 18 USC section 1734.

indicated days after the implantation, digital images of the corneal vessels were obtained and recorded using OpenLab software Version 2.2.5 (Improvision Inc) with standardized illumination and contrast.

Site-specific patterns of GF-induced angio- and lymphangiogenesis

Using the corneal pocket assay,[20] a GF-containing pellet was implanted into corneal stroma at 12 o'clock. The GF diffuses into the corneal stroma, and its concentration presumably decreases with the distance from the pellet, creating a concentration gradient at the various sites in the cornea.[3] Thus, the GF concentration is considered lower in the sides (at 3 and 9 o'clock), compared with the front, and lowest in the back site of the cornea (at 6 o'clock).

Quantification of angiogenesis and lymphangiogenesis in whole-mount immunofluorescence

The eyes were enucleated and fixed with 4% paraformaldehyde for 30 minutes at 4°C. For whole-mount preparation, the corneas were microsurgically exposed by removing other portions of the eye. Tissues were washed with phosphate-buffered saline (PBS) 3× for 5 minutes and then placed in methanol for 20 minutes. Tissues were incubated overnight at 4°C with α-mouse CD31 monoclonal antibody (mAb; 5 μg/mL, 550274; BD Pharmingen), α-mouse LYVE-1 Ab (4 μg/mL, 103-PA50AG; RELIATech GmbH), and α-mouse VEGFR-2 Ab (20 μg/mL, AF644; R&D Systems) diluted in PBS containing 10% goat serum and 1% Triton X-100. Tissues were washed 4 times for 20 minutes in PBS followed by incubation with Alexa Fluor488 goat α-rat immunoglobulin (Ig)G (20 μg/mL, 52955A; Invitrogen) and Alexa Fluor647 goat α-rabbit IgG (20 μg/mL, A21244; Invitrogen) overnight at 4°C. Radial cuts were then made in the peripheral retina and cornea to allow flat mounting on a glass slide using a mounting medium (TA-030-FM, Mountant Permafluor; Lab Vision Corporation). The flat-mounted tissues were examined by fluorescence microscopy and recorded using OpenLab software Version 2.2.5 (Improvision Inc) with standardized illumination and contrast and were saved onto disks.

Immunohistochemistry

The eyes were harvested and snap-frozen in optimal cutting temperature compound (Sakura Finetechnical). Sections (10 μm) were prepared, air-dried, and fixed in ice-cold acetone for 10 minutes. The sections were blocked with 3% nonfat dried Milk bovine working solution (M7409; Sigma-Aldrich) and stained with α-mouse CD45 mAb (1:50, 550539; BD Pharmingen), α-mouse F4/80 mAb (1:100, MCA497R; Serotec), α-mouse CD31 mAb (1:50, 550274; BD Pharmingen), α-VEGF-C Ab (1:200, sc-7132; Santa Cruz Biotechnology), and α-mouse LYVE-1 Ab (1 μg/mL, 103-PA50AG; RELIAtech GmbH). After an overnight incubation, sections were washed and stained for 20 minutes with goat α-rat IgG CY5 conjugate (10 μg/mL, 81-9516; Zymed Labo), Alexa Fluor488 donkey α-goat IgG (10 μg/mL, A-11 055; Invitrogen), and Alexa Fluor647 goat α-rabbit IgG (20 μg/mL, A21244; Invitrogen).

Cell culture

Human umbilical vein endothelial cells (HUVECs; PromoCell; C-12 200 or Cambrex) were routinely cultured in endothelial cell growth medium-2 KIT (PromoCell; C-22111) supplemented with 2% fetal bovine serum (FBS) in a humidified incubator under 5% CO_2 at 37°C.

ELISA of VEGF-C and shed VEGFR-2 in HUVECs

HUVECS were starved for 12 hours and then stimulated with 20 ng/mL VEGF-A for 24 hours at 37°C. The supernatant was removed and the cells rinsed with ice-cold PBS. Subsequently, the cells were lysed using a mammalian cell lysis kit (MCL1; Sigma-Aldrich). VEGF-C concentration was measured using an enzymed-linked immunosorbent assay (ELISA) kit (BMS626; Bender MedSystems).

Real-time PCR

After starvation for 12 hours in 1% FBS medium, HUVECs were stimulated with 20 ng/mL VEGF-A for 24 hours at 37°C. Total RNA was extracted from HUVECs by Trizol Reagent (15 596-026; Invitrogen). RNA samples (2 μg) were transcribed to cDNA with the Reverse Transcription reagents (N808-0234; Applied Biosystems). Real-time polymerase chain reaction (PCR; using 100 ng cDNA) was performed using Step One Plus Real-Time PCR System and hVEGFR-2–specific TaqMan Gene Expression Assays for individual mRNAs (Hs00176676_m1) according to the manufacturer's protocol (Applied Biosystems).

Flow cytometry

After starvation for 12 hours in 1% FBS medium, HUVECs were stimulated with 20 ng/mL VEGF-A (497-MV; R&D Systems) for 24 hours at 37°C. HUVECs were harvested with 0.05% trypsin and washed with PBS. The cells were resuspended in PBS at a concentration of 10^7 cells/mL. Subsequently, the cell suspension was incubated with α-human VEGFR-2 mAbs (25 μg/mL, MAB3572; R&D Systems) for 15 minutes at room temperature. Cells were then washed twice with PBS and analyzed in a flow cytometer. As a control, a nonimmune mAb was used at the same concentration.

Western blotting

At day 6 after VEGF-A (400 ng) implantation into 4 corneas or after 24 hours incubation of VEGF-A (20 ng/mL), HUVECs were harvested in a mammalian cell lysis kit (MCL1; Sigma-Aldrich). Lysates were subjected to sodium dodecyl sulfate-polyacrylamide gel electrophoresis and transferred to Immobilon membranes (Millipore). Blots were incubated with α-mouse VEGFR-2 (0.2 μg/mL, AF644; R&D Systems), α-VEGF-C (1:200, sc-25 783; Santa Cruz Biotechnology), or α-β-tubulin (1:1000, ab11308; Abcam) and visualized with a secondary Ab coupled to horseradish peroxidase (Amersham) and enhanced chemiluminescence system.

Confocal laser scanning microscopy

After HUVECs were washed with PBS, cells were fixed with 4% formaldehyde in PBS and permeabilized in PBS containing 0.1% saponin. After washing with PBS, cells were blocked with 5% skim milk in PBS. Cells were incubated with VEGF-C Ab (1:50, sc-25 783; Santa Cruz Biotechnology), phospho VEGFR-2 Ab (1:100, sc-16 628; Santa Cruz Biotechnology) overnight at 4°C. Subsequently, Alexa Fluor 488-conjugated and 555-conjugated second Ab (1:200) was used for 1 hour at room temperature. Fluorescence images were observed on a Zeiss LSM 510 META confocal laser scanning microscope (Carl Zeiss). Three-dimensional data were analyzed by LSM 510 software.

Proliferation assay

HUVECs were suspended in complete medium and plated at 4×10^3 cells/well in 96-well plates and incubated at 37°C for 48 hours. Soluble tetrazolium salt (MTS) assay was performed according to the manufacturer's protocol (G5421, Promega). Briefly, 30 μL of MTS reagent was added to each well (100 μL of medium) and incubated at 37°C for 2 hours. The absorbance was then measured at 490 nm.

In vivo molecular imaging and preparation of probes

Recently, we introduced a novel technique for detection of endothelial surface molecules in acute ocular inflammation.[21,22] Using adhesion molecule–conjugated fluorescent microspheres (MSs)[23] in live animals, we showed early endothelial changes in ocular microvessels at an early stage, one that was previously only detectable by the most sensitive in vitro techniques, such as immunohistochemistry or PCR.[22] To prepare the imaging probes, carboxylated fluorescent or nonfluorescent MSs (2 μm, Polysciences Inc) were covalently conjugated to protein G (Sigma-Aldrich), using a carbodiimide-coupling kit (Polysciences Inc).[24] α-mouse VEGFR-1 Ab (sc-9029; Santa Cruz Biotechnology), α-mouse VEGFR-2 Ab (AF644; R&D Systems), or control goat IgG (AB-108-C; R&D

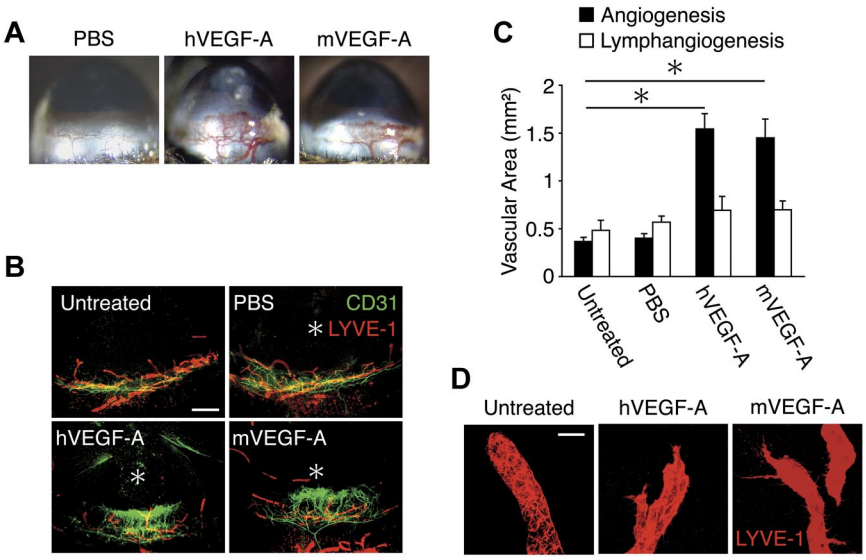

Figure 1. VEGF-A–induced lymph- and angiogenesis. Pellets containing hVEGF (200 ng) or mVEGF-A (200 ng) were implanted into the corneas of C57BL/6 mice. Corneal lymph- and angiogenesis were examined on day 6 after implantation. (A) Microscopic pictures of corneal neovascularization. (B) Double staining of corneal flat mounts for angiogenesis (CD31) and lymphangiogenesis (LYVE-1). *Implanted pellets. Bar, 400 μm. (C) Quantitative analysis of vascular area (black) and lymphatic area (white; n = 4-8). (D) Blind round tips of lymphatics in normal corneas and branched sharp tips in VEGF-A–stimulated corneas of confocal images. Bar, 30 μm. *$P < .05$.

Systems) was incubated with the MSs at 0.4 mg/mL overnight at room temperature. MSs were washed in PBS with 1% bovine serum albumin before use in vivo. Then, 6×10^7 fluorescent MSs were injected in each mouse. After systemic injection, the interactions of these MSs with the endothelium of normal and angiogenic vessels of live animals was studied by intravital video microscopy.[24]

Statistical analysis

All values are expressed as mean plus or minus SEM. Data were analyzed by Student *t* test. Differences between the experimental groups were considered statistically significant or highly significant, when the probability value, *P*, was $< .05$ or $< .01$, respectively.

Results

VEGF-A–induced lymph- and angiogenesis

To investigate the lymph- and angiogenic potential of VEGF-A, we implanted hVEGF-A (200 ng) or mVEGF-A (200 ng) in corneas of mice. hVEGF-A (200 ng) and mVEGF-A (200 ng) induced significant angiogenesis on day 6 (Figure 1A). To examine whether VEGF-A induces lymphangiogenesis, we performed immunohistochemistry in corneal flat mounts with α-CD31 and α-LYVE-1 Abs. The lymphatic area in hVEGF-A as well as mVEGF-A–implanted corneas did not differ from PBS-implanted corneas (Figure 1B-C). In confirmation of our recent report,[4] pre-existing blind-ended lymphatic vessels were found above the limbal vascular loops in untreated corneas (Figure 1B,D). In contrast to the round tips of the pre-existing lymphatics, the newly growing lymphatics in both hVEGF-A– and mVEGF-A–implanted corneas showed pointy endings (Figure 1D). These data indicate that 200 ng VEGF-A induces lymphatic sprouting but does not increase the area of lymphatics.

Different dose thresholds for VEGF-A–induced lymph- and angiogenesis

To explore whether differences in dose thresholds underlie the differential lymphangiogenic responses at the various corneal sites, we implanted various VEGF-A doses (25, 100, 400, and 1600 ng) into the mouse corneas. Corneal angiogenesis occurred in 100, 400, and 1600 ng VEGF-A–implanted corneas, but not 25 ng, suggesting the dose threshold for corneal angiogenesis to be approximately 100 ng (Figure 2A-B). The 100 ng VEGF-A induced significant angiogenesis but not lymphangiogenesis, while 400 and 1600 ng VEGF-A induced both lymph- and angiogenesis, suggesting the dose threshold for VEGF-A–induced corneal lymphangiogenesis to be higher than angiogenesis (Figure 2A-B). Furthermore, 400 and 1600 ng but not 100 ng VEGF-A increased the number of lymphatic tips compared with control (Figure 2A,C). In 400 ng or 1600 ng VEGF-A–implanted corneas, the portion of the lymphatic tips was similar to that of angiogenic tips (Figure 2A,D). These data indicate that the dose of VEGF-A, which causes lymphangiogenesis, is not sufficient to cause their growth beyond angiogenic vessels. Furthermore, there was no lymphangiogenesis without angiogenesis in the side and back of the VEGF-A–implanted corneas at the various doses (Figure 2A,E). These data indicate different thresholds for VEGF-A–induced lymph- and angiogenesis.

Differential temporal lymph- and angiogenic responses to VEGF-A

To examine the time course of VEGF-A–induced lymph- and angiogenesis, we implanted VEGF-A and followed vessel growth for 14 days. Dilation of the blood vessels was present on day 2, and sprouting on day 4 and between day 10 and 14 angiogenic vessels reached the site of cytokine implantation (Figure 3A). The area of VEGF-A–induced angiogenesis was significantly larger on day 4, 6, 10, and 14 but not day 2, compared with PBS (Figure 3A,B). VEGF-A–induced lymphangiogenic area on day 10 and 14 but not on day 4 and 6 were larger than PBS control (Figure 3A-B). Interestingly, lymphangiogenic area on day 2 was lower than PBS-implanted on day 6 (Figure 3A-B). The number of lymphatic tips was significantly increased on day 6, 10, and 14 after VEGF-A stimulation (Figure 3C). On day 14, well-branched lymphangiogenesis was observed in VEGF-A–implanted corneas (Figure 3A). Furthermore, the number of lymphatics in the side and back of the VEGF-A–implanted corneas on day 10 and 14 was significantly higher than control (Figure 3A,D). These data indicate that VEGF-A–induced angiogenesis peaks earlier than lymphangiogenesis. Furthermore, to show the relation between lymph- and angiogenesis by VEGF-A, the ratio of length of angiogenic vessels

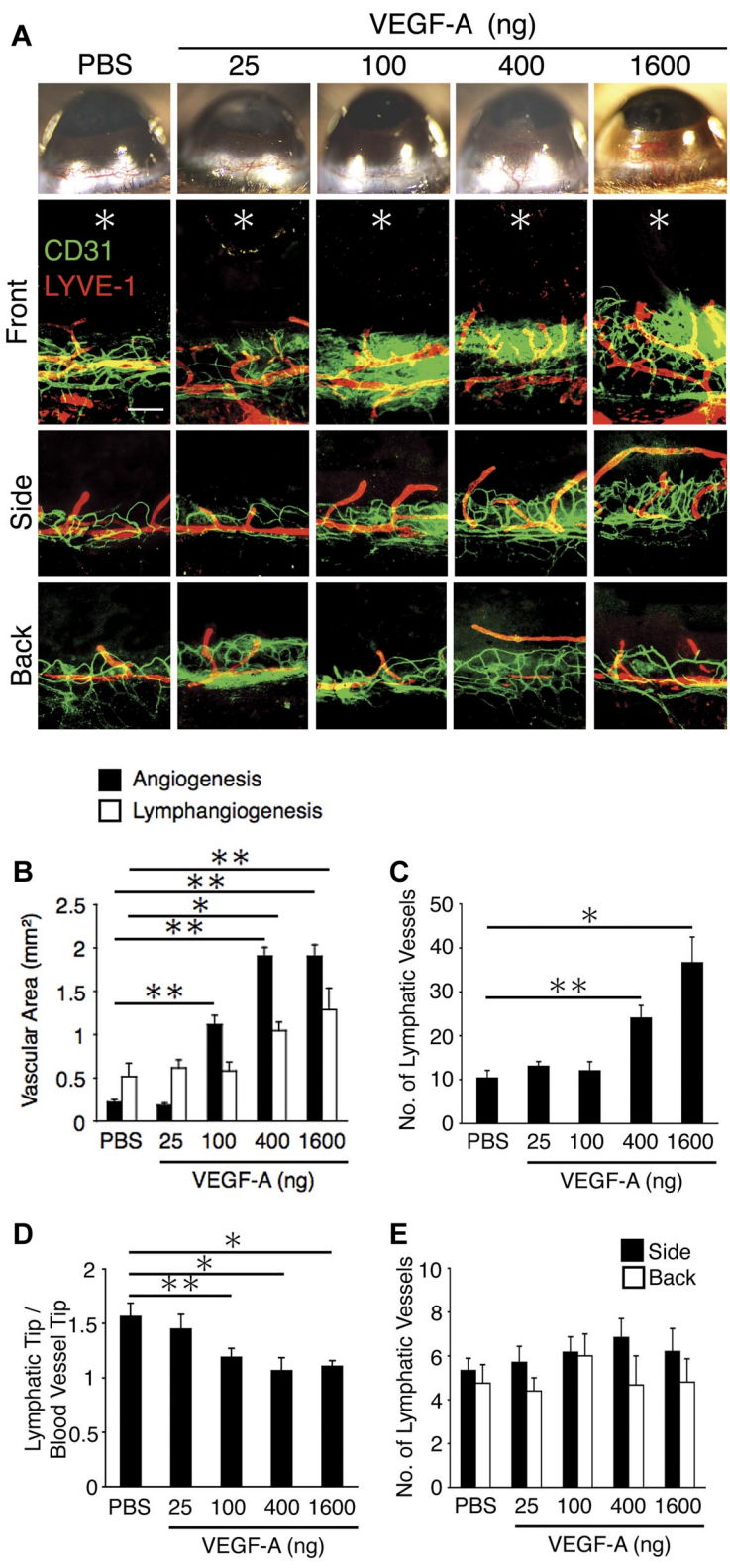

Figure 2. VEGF-A–concentration dependent corneal angiogenesis and lymphangiogenesis. Control pellets (PBS) or pellets with varying amounts of VEGF-A (25, 100, 400, and 1600 ng) were implanted into the corneas of C57BL/6 mice. Corneal angiogenesis and lymphangiogenesis were examined on day 6 after pellet implantation. (A) Double staining of corneal flat mounts for angiogenesis (CD31, green) and lymphangiogenesis (LYVE-1, red) in the front, side, and the back of the cornea. *Implanted pellets. Bar, 200 μm. (B) Quantitative analysis of angiogenesis and lymphangiogenesis on day 6 (n = 5-8). (C) Quantitation of the number of LYVE-1(+) lymphatic vessels in corneas of PBS or VEGF-A– (25, 100, 400, or 1600 ng) implanted animals (n = 5-6). (D) Ratio of the distance of lymphatic tips and vascular tips from limbal vessels in corneas of PBS or VEGF-A– (25, 100, 400, or 1600 ng) implanted animals (n = 15-22). (E) Quantitation of the number of lymphatic vessels (n = 4-10). Bar, 200 μm. *$P < .05$; **$P < .01$.

and lymphangiogenic vessels was examined. On days 4, 6, 10, and 14, the ratio was smaller than control, as the angiogenic vessels approached the leading edge of the pre-existing lymphatic vessels (Figure 3E). These data indicate that the pre-existing lymphatic vessels first start to grow, when the angiogenic vessels have passed them, albeit sprouting of the lymphatic endothelium does occur before then.

Contribution of VEGF-C and VEGFR-3 to VEGF-A–induced lymphangiogenesis

To investigate the mechanisms underlying delayed lymphangiogenesis relative to angiogenesis, we measured VEGF-C expression in VEGF-A–implanted corneas. Immunohistochemistry with an α-VEGF-C Ab showed that CD31(+) vascular endothelial cells as

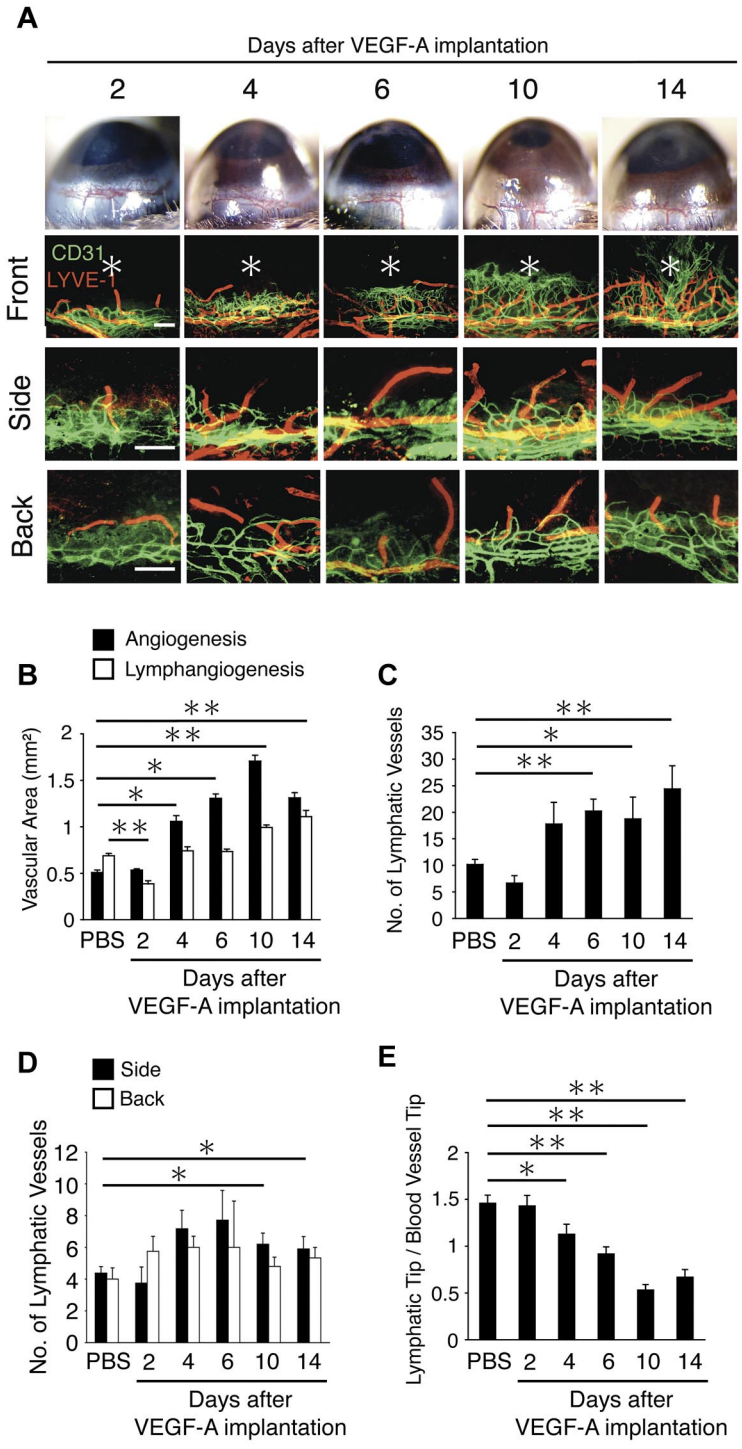

Figure 3. Time course of VEGF-A–dependent corneal lymph- and angiogenesis. (A) Double staining of corneal flat mounts for lymph- (LYVE-1, red) and angiogenesis (CD31, green) in the front, side, and the back of the cornea. Bar, 200 μm. (B) Quantitative analysis of lymph- and angiogenesis on the indicated day after VEGF-A implantation (n = 4-8). (C) Quantitation of the number of LYVE-1(+) lymphatic vessels in corneas of PBS or VEGF-A–implanted animals (n = 4-6). (D) Ratio of the distance of lymphatic tips and vascular tips from limbal vessels in corneas of PBS or VEGF-A–implanted animals (n = 12-18). (E) Quantitation of the number of lymphatic vessels (n = 4-10). Bar, 200 μm. *$P < .05$; **$P < .01$.

well as CD45(+)/F4/80(+) leukocytes expressed VEGF-C in VEGF-A–implanted corneas (Figure 4A). These data indicate that the source of VEGF-C in VEGF-A–induced lymphangiogenesis is not only leukocytes, especially macrophages but also vascular endothelial cells. VEGFR-3 was expressed in VEGF-A–induced lymphatics (Figure 4B). VEGF-C was up-regulated in VEGF-A–implanted corneas compared with PBS-implanted controls (Figure 4C).

To understand the extent of VEGF-C's contribution to VEGF-A–induced lymphangiogenesis, we treated VEGF-A–implanted corneas with soluble VEGFR-3 (sR3). VEGF-C inhibition significantly reduced the number of lymphatic tips and inhibited lymphatic sproutings in VEGF-A–implanted corneas compared with control (Figure 4D-E). These data indicate that VEGF-C contributes to lymphatic sprouting in VEGF-A–induced lymphangiogenesis.

VEGF-A–induced VEGF-C up-regulation in blood vessel endothelium guides lymphatic growth

In VEGF-A–implanted corneas, we made the surprising observation that not all lymphangiogenic tips oriented themselves toward the GF-containing pellets, as a significant portion of the tips sprouted in the opposite direction, toward the blood vessels (Figure

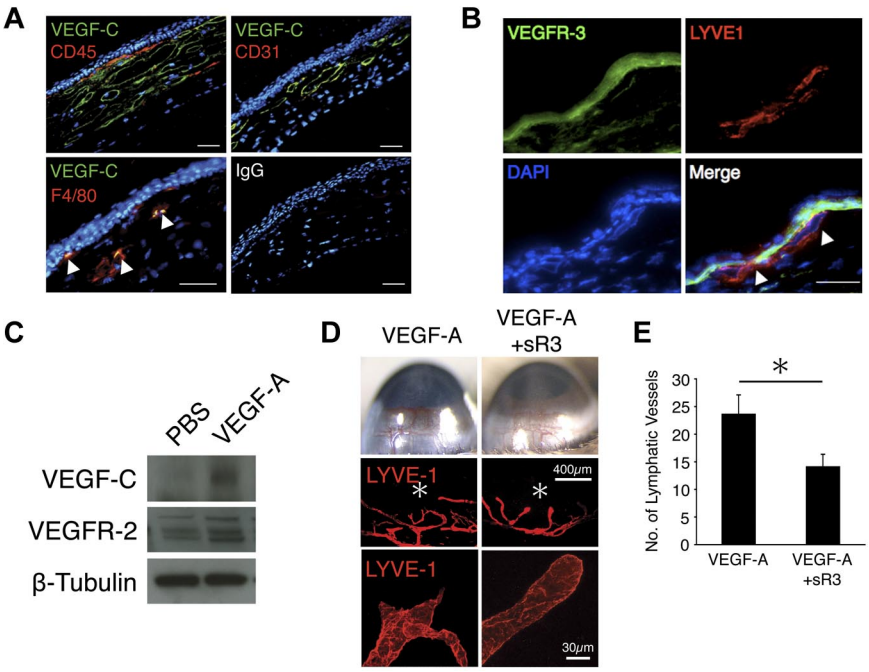

Figure 4. Contribution of VEGFR-3 to VEGF-A–induced lymphangiogenesis. Corneas were implanted with pellets containing VEGF-A (200 ng). Corneal sections were examined on day 6 after implantation. (A) Double immunostaining of corneal sections with VEGF-C (green) and CD45 (red), CD31 (red), or F4/80 (red). Bar, 50 μm. (B) Double immunostaining of VEGF-A–implanted corneal sections with VEGFR-3 (green) and LYVE-1 (red). Arrowheads indicate VEGFR-3–positive lymphatic endothelium. Bar, 50 μm. (C) Representative Western blot of samples of PBS or VEGF-A–implanted corneas (day 6) with Abs of VEGF-C, VEGFR-2, or β-tubulin. (D) Pellets containing VEGF-A or VEGF-A+sR3 were implanted into the corneas of C57BL/6 mice (day 6). *Pellet implantation site. LYVE-1 (red). (E) Quantitation of the number of lymphatic vessels in VEGF-A–implanted corneas with or without sR3 on day 6 (n = 6-8). *$P < .05$.

5A-B). Notably, tips of the pre-existing lymphatics that were beyond the vascular plexus were round, whereas the shape of the lymphatics in the vicinity of the blood vessels were pointy (Figure 5A). To examine whether blood vesse–derived VEGF-C guides the lymphatic sprouts in VEGF-A over-expression, we examined lymphatic tip direction in VEGF-A–, VEGF-C–, and VEGF-A/VEGF-C–double implanted corneas. VEGF-C co-implantation with VEGF-A significantly reduced the portion of the sprouting lymphatic tips that grew toward the angiogenic vessels, indicating that endothelial VEGF-C up-regulation by VEGF-A underlies lymphatic tip sprouting (Figure 5C-D).

This observation led to the hypothesis that vascular endothelium–derived VEGF-C may regulate VEGF-A–induced lymphangiogenic tip sprouting. To examine whether VEGF-A induces VEGF-C expression in endothelial cells, we measured in ELISA VEGF-C protein expression in VEGF-A–stimulated HUVECs. VEGF-C expression was significantly induced by VEGF-A in the whole cell lysates of HUVECs (Figure 6A). Surprisingly, VEGF-C level in the supernatant of VEGF-A–stimulated HUVECs was significantly lower than unstimulated HUVECs (Figure 6B). Reverse-transcription PCR showed a 1.7-fold increase in the VEGF-C mRNA level after VEGF-A stimulation. These data suggest that VEGF-A–induced lymphangiogenesis is regulated through vascular endothelial derived VEGF-C.

Surprising impact of blood vessel endothelial VEGFR-2 on VEGF-A–induced lymphangiogenesis: an endogenous VEGF-C trapping mechanism regulates lymphangiogenesis

We hypothesized that VEGFR-2 on vascular endothelium may trap VEGF-A–induced VEGF-C and therewith cause delayed lymphangiogenesis in response to VEGF-A. To address this, we

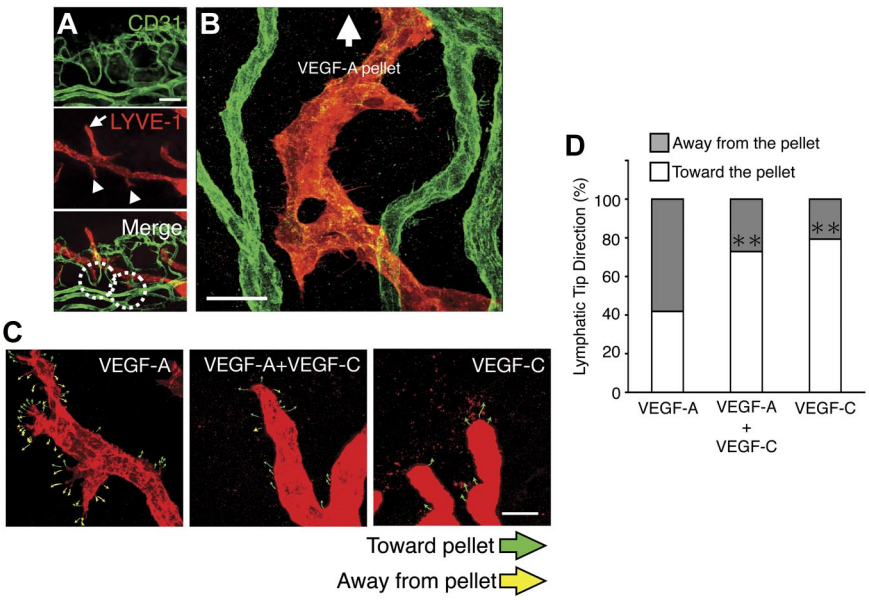

Figure 5. Angiogenic vessel derived VEGF-C regulates VEGF-A–induced lymphatic sprouting. (A) Double staining of corneal flat mounts for lymph- (LYVE-1) and angiogenesis (CD31) on day 4 after VEGF-A implantation. Arrowheads indicate descending lymphatic tips toward vascular vessels. Arrows indicate round tips of lymphatics over vascular plexus. Bar, 100 μm. (B) Confocal image illustrates descending lymphatic tips and lymphatics toward blood vessels on day 10 after VEGF-A implantation. Bar, 30 μm. (C-D) Lymphatic tip direction of VEGF-A, VEGF-C, or VEGF-A+VEGF-C mixture–induced lymphatics on day 6 (C). White symbols indicate tips toward GF pellet, and gray symbols indicate tips away from the pellet and percent of tips (D; n = 5-7). **$P < .01$.

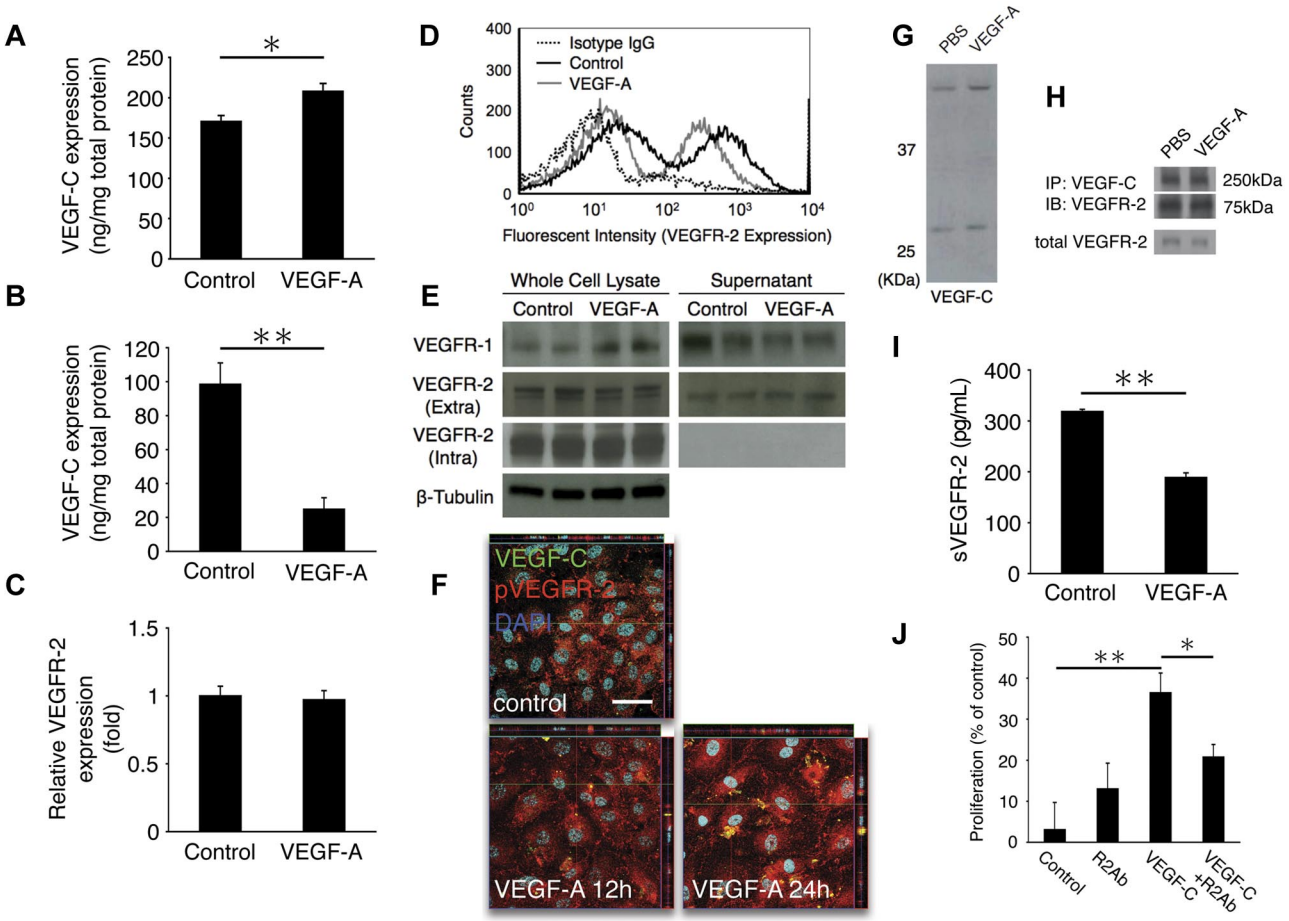

Figure 6. Regulatory role of VEGFR-2 in VEGF-A–induced lymphangiogenesis. (A-B) VEGF-C expression with VEGF-A stimulation in whole cell lysates (A) and supernatant (B) of HUVECs, measured with ELISA (n = 4 [A] and 8 [B]). (C) VEGFR-2 mRNA level at 24 hours after VEGF-A stimulation is similar with control. (D) Flow cytometric analysis of VEGFR-2 expression in normal and VEGF-A–treated HUVECs, showing R2 down-regulation with VEGF-A stimulation at 24 hours. (E) Western blots of VEGFRs expression in whole cell lysates and supernatants of HUVECs with or without VEGF-A (24-hour treatment). (F) Confocal images of immunocytochemistry of phospho-VEGFR-2 (red) and VEGF-C (green) with or without VEGF-A stimulation (12 and 24 hours) in HUVECs. Arrows indicate pVEGFR-2/VEGF-C complex in the cytoplasm. Bar, 50 μm. (G) Representative Western blot samples from untreated and VEGF-A–treated HUVECs with α-VEGF-C Ab, showing up-regulation of precursor and secreted form of VEGF-C with VEGF-A. (H) Immunoprecipitated (IP) with VEGF-C and immunoblotted with VEGFR-2 Ab. tVEGFR-2 shows total VEGFR-2 without IP. (I) Soluble VEGFR-2 expression in VEGF-A–stimulated supernatant of HUVECs, measured with ELISA (n = 4). (J) VEGF-C–induced proliferation of HUVECs treated with IgG or VEGFR-2 Ab. Proliferation was measured at day 2 using the MTS assay (optical density at 490 nm). *$P < .05$; **$P < .01$.

measured the expression level of VEGFR-2 in HUVECs with or without VEGF-A stimulation by FACS, Western blotting, and reverse-transcription PCR. VEGFR-2 was down-regulated on the surface of HUVECs (Figure 6D), whereas VEGFR-2 mRNA and protein levels of whole-cell lysates in VEGF-A–treated HUVECs were similar to control (Figure 6C,E), suggesting either removal or internalization of VEGFR-2 from the surface.

To investigate whether VEGF-A stimulation causes internalization of VEGF-C bound to VEGFR-2, we performed confocal microscopy of VEGFR-2 and VEGF-C upon VEGF-A treatment in HUVECs. At 12 and 24 hours after VEGF-A stimulation, more phosphorylated VEGFR-2 and VEGF-C complexes were found in VEGF-A–treated cells than in controls (Figure 6F). To examine, whether the VEGFR-2/VEGF-C complex is affected by VEGF-A stimulation, we performed immunoprecipitation with α-VEGF-C Ab and immunoblotted with α-VEGFR-2 Ab. Western blots showed that VEGF-C was up-regulated by VEGF-A (Figure 6G). The VEGFR-2/VEGF-C complex was detected in whole cell lysates of untreated and VEGF-A–treated HUVECs; however, the amount of the complex (75 kDa and 250 kDa) was unaffected by VEGF-A stimulation (Figure 6H). These data suggest that VEGF-A causes internalization of the phosphorylated VEGFR-2/VEGF-C complex and that degradation of the complex may follow after internalization.

To investigate whether sVEGFR-2 traps VEGF-C, we measured VEGFR-2 in the whole cell lysate and supernatant of HUVECs with a VEGFR-2 mAb that detects the extracellular domain. In line with a previous report,[25] sVEGFR-2 was detected in the supernatant of HUVECs; however, it was surprisingly reduced with VEGF-A treatment, in line with our internalization hypothesis (Figure 6I). We also confirmed that the ELISA detects free soluble VEGFR-2 and ligand-bound soluble VEGFR-2 equally because VEGF-A treatment did not change the detected concentration (supplemental Figure 1, available on the *Blood* Web site; see the Supplemental Materials link at the top of the online article). These data indicate that total sVEGFR-2 is down-regulated by VEGF-A stimulation. Furthermore, there was no VEGFR-2/VEGF-C complex detectable in the supernatant. To investigate whether VEGF-C contributes to angiogenesis via blood endothelial cell proliferation, we treated HUVECs with VEGF-C with or without a VEGFR-2 neutralizing Ab and measured cell proliferation in the MTS assay. VEGF-C induced proliferation of the HUVECs, and the induction

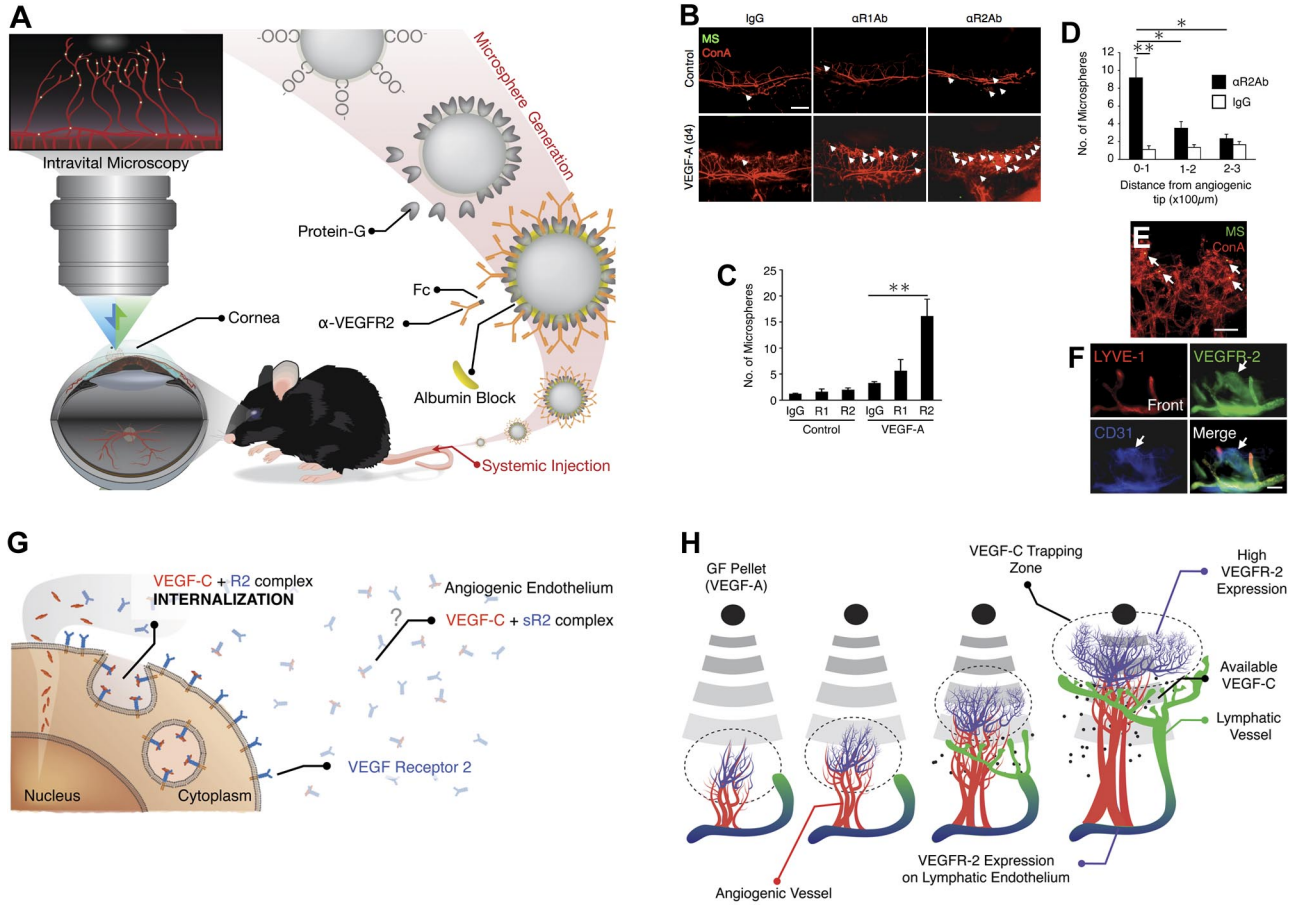

Figure 7. In vivo molecular imaging of VEGFR-2 in VEGF-A–induced angiogenesis. (A) Schematic of our in vivo molecular imaging approach to study VEGFR-2 expression in corneal angiogenic vessels. Fluorescent MSs conjugated with anti-VEGFRs Ab are injected systemically in live animals. (B) α-VEGFRs mAb–conjugated MSs (green) and rhodamin-conjugated conA (red). Arrows indicate MS in blood vessels. Bar, 200 μm. (C) Quantitation of the number of α-VEGFRs Abs-conjugated MS in corneal vessels of untreated and VEGF-A–implanted eyes (day 4; n = 4-12). (D) Distribution of α-VEGFR-2 Ab-conjugated MS or IgG-conjugated MS in VEGF-A–induced angiogenesis (day 4). (E) Representative confocal image (100× objective) of a corneal flatmount on day 6 after VEGF-A implantation. For in vivo molecular imaging of VEGFR-2, animals were injected with α-VEGFR-2 mAb–conjugated MS (green) and 30 minutes later perfused with rhodamin-conjugated conA (red) to stain the vasculature. Bar, 30 μm. (F) Triple staining for LYVE-1 (red), VEGFR-2 (green), and CD31 (blue) in the front of VEGF-A– implanted corneas (day 6). Bar, 100 μm. *$P < .05$; **$P < .01$. (G) Angiogenic endothelium expressed higher levels of VEGFR-2 that actively traps VEGF-C on the endothelial surface. Subsequently, the VEGFR-2/VEGF-C complex is internalized and therewith cleared from the extracellular matrix. (H) Mechanism of delayed lymphangiogenesis. Sprouting blood vessel endothelium expresses VEGFR-2 and VEGF-C. Lymphatic endothelium expresses VEGFR-2 and -3 but not VEGF-C. The endothelium of the angiogenic tip VEGF-C is trapped by VEGFR-2 and internalized. In a distance from the angiogenic tips and in absence of the active trapping mechanism, blood endothelial–derived VEGF-C reaches lymphatic endothelium, allowing their growth.

was inhibited by VEGFR-2 inhibition (Figure 6J). These data suggest that VEGF-C signaling through VEGFR-2 contributes to blood vessel growth.

In vivo molecular imaging reveals elevated VEGFR-2 expression

To investigate whether VEGFR-2 contributes to VEGF-A–induced corneal lymphangiogenesis, we quantified VEGFR-2 expression. Western blots showed higher VEGFR-2 expression in VEGF-A–implanted corneas compared with PBS-implanted controls (Figure 4C). In vivo expression of the VEGFR-2 in blood vessel endothelium in response to VEGF-A stimulation was quantified using our molecular imaging technique with α-VEGFR Ab-conjugated MSs (Figure 7A).[21,22,24] The number of accumulated α-VEGFR-2 Ab- but not α-VEGFR-1 Ab-conjugated MSs in the vasculature of VEGF-A–implanted corneas was significantly higher than in untreated controls (Figure 7B-C and supplemental Videos 2,4). Notably, α-VEGFR-2 Ab-conjugated MSs were detected around the angiogenic tips, more than in the angiogenic stalks (Figure 7B,D). Control IgG-conjugated MSs showed low numbers of interactions with the vascular endothelium of normal or VEGF-A–implanted animals (supplemental Videos 1,3). Confocal microscopy showed that the MSs were indeed inside of the lumen of the angiogenic vessels (Figure 7E). Furthermore, immunostaining showed VEGFR-2 expression in angiogenic vessels in VEGF-A–implanted corneas (Figure 7F).

Discussion

The poised temporal and spatial association of angio- and lymphangiogenesis suggests intricate interdependencies between blood and lymphatic vessels. In response to GFs, such as VEGF-A, lymphatics grow with a delay compared with blood vessels. Furthermore, higher concentrations of these GFs are needed for lymphangiogenesis than for angiogenesis. However, how these vessel types might influence each other was previously unknown.

Our results indicate that VEGF-C derived from blood vessel guides lymphatic sprouting and growth. The paradoxical orientation of lymphatic sprouting away from VEGF-A pellets toward the blood vessels shows the critical role of blood vessel–derived factors in lymphatic growth. Exogenous VEGF-C overrides this

phenomenon, underlining this critical role that initiates lymphatic guidance. SR3 effectively reduces VEGF-A–induced lymphangiogenesis, indicating the key role of VEGF-C (and potentially VEGF-D) in VEGF-A–induced lymphangiogenesis.

The unexpected finding of lower VEGF-C in the supernatant of VEGF-A–treated endothelial cells led us to propose a clearance mechanism for VEGF-C during angiogenesis. Receptor-mediated internalization is a fundamental biological principle that regulates key functions;[26] however, GF-clearance through this pathway, including vascular growth regulation, was unknown. VEGFR-2, a VEGF-C receptor,[8] is up-regulated on blood vessel endothelium in response to pro-angiogenic GFs.[27] VEGF-C binding to endothelial VEGFR-2 would not only have an autocrine effect but also a reduction of the VEGF-C concentration in the extracellular matrix. Thus, VEGFR-2 binding to VEGF-C would act as an endogenous trapping mechanism and suppress lymphatic growth (Figure 7G). In support of this model, in VEGF-A–stimulated HUVECs, the VEGF-C/VEGFR-2 complex is found in the cytoplasm, indicating internalization of the captured VEGF-C by VEGFR-2 (Figure 7G).

In the forefront of the angiogenic field, our in vivo molecular imaging reveals highest VEGFR-2 expression in the angiogenic tips, which would maximize the autocrine function of the GFs in the growing blood vessels. Especially in these areas, the lymphatic growth is most impeded. Analogously, VEGFR-3 is higher in tumor angiogenesis and during wound healing,[28,29] where it could potentially regulate lymphangiogenesis.

Further puzzling is the lower concentration threshold for GF-induced angiogenesis, compared with lymphangiogenesis. Both blood vessel endothelium and lymphatic endothelium express VEGFR-2; however, lower VEGF-A concentrations only cause blood vessel growth. We show that VEGF-C– (or VEGF-D)–mediated signaling is necessary for lymphatic growth, as sR3 suppresses VEGF-A–induced lymphangiogenesis. This suggests that, despite the direct interaction of VEGF-A with the lymphatic endothelium, its growth depends on the blood vessel–generated VEGF-C (or VEGF-D).

This work elucidates a previously unknown link that finely regulates lymphatic growth in spatial and temporal relation to angiogenic vessels. We show VEGF-C trapping by endothelial VEGFR-2 as an example for GFs clearance from the extracellular matrix through receptor-mediated internalization. Angiogenic vessels use this previously unknown mechanism to regulate their environment, such as the growth of lymphatics. An imbalance between the blood and lymphatic growth could impact tissue homeostasis, immunity, or cancer growth and spreading.

Acknowledgments

We thank Lama Almulki, Sepideh Faez, Toshio Hisatomi, Shinsuke Miyahara, Toru Nakazawa, Kousuke Noda, Mahdi Taher, Faryan Tayyari, and Fang Xie for technical assistance and insightful discussions.

This work was supported by National Institutes of Health grant AI050775 (AH-M), an overseas Research Fellowship Award from Bausch and Lomb, a Fellowship Award from the Japan Eye Bank Association and Tear Film and Ocular Surface Society and Young Investigator Fellowship, the American Health Assistance Foundation, and the Malaysian Palm Oil Board.

Authorship

Contribution: S.N. and A.H.-M. designed research and organized the experiments; A.H.-M., S.N., S.Z., Y.H., S.K., R.A., A.S., D.S., M.I.M., Y.I., and N.L.-C. performed research and analyzed data; and S.N. and A.H.-M. wrote the paper.

Conflict-of-interest disclosure: The authors declare no competing financial interests.

The current affiliation for A.H.-M., M.I.M., D.S., A.S., and S.Z. is Center for Excellence in Functional and Molecular Imaging, Brigham and Women's Hospital, Department of Radiology, Harvard Medical School, Boston, MA.

Correspondence: Ali Hafezi-Moghadam, Brigham and Women's Hospital, Center for Excellence in Functional and Molecular Imaging, 221 Longwood Ave, 3rd Fl, Boston, MA 02115; e-mail: AHM@BWH.harvard.edu.

References

1. Karpanen T, Alitalo K. Molecular biology and pathology of lymphangiogenesis. *Annu Rev Pathol.* 2008;3:367-397.
2. Kriehuber E, Breiteneder-Geleff S, Groeger M, et al. Isolation and characterization of dermal lymphatic and blood endothelial cells reveal stable and functionally specialized cell lineages. *J Exp Med.* 2001;194(6):797-808.
3. Chang LK, Garcia-Cardena G, Farnebo F, et al. Dose-dependent response of FGF-2 for lymphangiogenesis. *Proc Natl Acad Sci U S A.* 2004; 101(32):11658-11663.
4. Nakao S, Maruyama K, Zandi S, et al. Lymphangiogenesis and angiogenesis: concurrence and/or dependence? Studies in inbred mouse strains. *FASEB J.* 2010;24(2):504-513.
5. Albuquerque RJ, Hayashi T, Cho WG, et al. Alternatively spliced vascular endothelial growth factor receptor-2 is an essential endogenous inhibitor of lymphatic vessel growth. *Nat Med.* 2009;15(9): 1023-1030.
6. Skobe M, Hawighorst T, Jackson DG, et al. Induction of tumor lymphangiogenesis by VEGF-C promotes breast cancer metastasis. *Nat Med.* 2001; 7(2):192-198.
7. Alitalo K, Mohla S, Ruoslahti E. Lymphangiogenesis and cancer: meeting report. *Cancer Res.* 2004;64(24):9225-9229.
8. Joukov V, Pajusola K, Kaipainen A, et al. A novel vascular endothelial growth factor, VEGF-C, is a ligand for the Flt4 (VEGFR-3) and KDR (VEGFR-2) receptor tyrosine kinases. *EMBO J.* 1996;15(7):1751.
9. Achen MG, Jeltsch M, Kukk E, et al. Vascular endothelial growth factor D (VEGF-D) is a ligand for the tyrosine kinases VEGF receptor 2 (Flk1) and VEGF receptor 3 (Flt4). *Proc Natl Acad Sci U S A.* 1998;95(2):548-553.
10. Joukov V, Sorsa T, Kumar V, et al. Proteolytic processing regulates receptor specificity and activity of VEGF-C. *Embo J.* 1997;16(13):3898-3911.
11. Cao Y, Linden P, Farnebo J, et al. Vascular endothelial growth factor C induces angiogenesis in vivo. *Proc Natl Acad Sci U S A.* 1998;95(24): 14389-14394.
12. Hirakawa S, Hong YK, Harvey N, et al. Identification of vascular lineage-specific genes by transcriptional profiling of isolated blood vascular and lymphatic endothelial cells. *Am J Pathol.* 2003; 162(2):575-586.
13. Dvorak HF, Brown LF, Detmar M, Dvorak AM. Vascular permeability factor/vascular endothelial growth factor, microvascular hyperpermeability, and angiogenesis. *Am J Pathol.* 1995;146(5): 1029-1039.
14. Nagy JA, Vasile E, Feng D, et al. Vascular permeability factor/vascular endothelial growth factor induces lymphangiogenesis as well as angiogenesis. *J Exp Med.* 2002;196(11):1497-1506.
15. Cursiefen C, Chen L, Borges LP, et al. VEGF-A stimulates lymphangiogenesis and hemangiogenesis in inflammatory neovascularization via macrophage recruitment. *J Clin Invest.* 2004; 113(7):1040-1050.
16. Hirakawa S, Kodama S, Kunstfeld R, Kajiya K, Brown LF, Detmar M. VEGF-A induces tumor and sentinel lymph node lymphangiogenesis and promotes lymphatic metastasis. *J Exp Med.* 2005; 201(7):1089-1099.
17. Ferrara N. Vascular endothelial growth factor. *Arterioscler Thromb Vasc Biol.* 2009;29(6):789-791.
18. Watari K, Nakao S, Fotovati A, et al. Role of macrophages in inflammatory lymphangiogenesis: Enhanced production of vascular endothelial growth factor C and D through NF-kappaB activation. *Biochem Biophys Res Commun.* 2008;377(3):826-831.
19. Baluk P, Tammela T, Ator E, et al. Pathogenesis of persistent lymphatic vessel hyperplasia in

chronic airway inflammation. *J Clin Invest.* 2005; 115(2):247-257.

20. Nakao S, Hata Y, Miura M, et al. Dexamethasone inhibits interleukin-1beta-induced corneal neovascularization: role of nuclear factor-kappaB-activated stromal cells in inflammatory angiogenesis. *Am J Pathol.* 2007;171(3): 1058-1065.
21. Miyahara S, Almulki L, Noda K, et al. In vivo imaging of endothelial injury in choriocapillaris during endotoxin-induced uveitis. *Faseb J.* 2008; 22(6):1973-1980.
22. Sun D, Nakao S, Xie F, Zandi S, Schering A, Hafezi-Moghadam A. Superior sensitivity of novel molecular imaging probe: simultaneously targeting two types of endothelial injury markers. *Faseb J.* 2010;24(5):1532-1540.
23. Hafezi-Moghadam A, Thomas KL, Prorock AJ, Huo Y, Ley K. L-selectin shedding regulates leukocyte recruitment. *J Exp Med.* 2001;193(7):863-872.
24. Hafezi-Moghadam A, Ley K. Relevance of L-selectin shedding for leukocyte rolling in vivo. *J Exp Med.* 1999;189(6):939-948.
25. Swendeman S, Mendelson K, Weskamp G, et al. VEGF-A stimulates ADAM17-dependent shedding of VEGFR2 and crosstalk between VEGFR2 and ERK signaling. *Circ Res.* 2008;103(9): 916-918.
26. Brown MS, Goldstein JL. Analysis of a mutant strain of human fibroblasts with a defect in the internalization of receptor-bound low density lipoprotein. *Cell.* 1976;9(4 PT 2):663-674.
27. Pettersson A, Nagy JA, Brown LF, et al. Heterogeneity of the angiogenic response induced in different normal adult tissues by vascular permeability factor/vascular endothelial growth factor. *Lab Invest.* 2000;80(1):99-115.
28. Valtola R, Salven P, Heikkila P, et al. VEGFR-3 and its ligand VEGF-C are associated with angiogenesis in breast cancer. *Am J Pathol.* 1999; 154(5):1381-1390.
29. Paavonen K, Puolakkainen P, Jussila L, Jahkola T, Alitalo K. Vascular endothelial growth factor receptor-3 in lymphangiogenesis in wound healing. *Am J Pathol.* 2000;156(5):1499-1504.

2011 117: 1081-1090
doi:10.1182/blood-2010-02-267427 originally published online August 12, 2010

Blood vessel endothelial VEGFR-2 delays lymphangiogenesis: an endogenous trapping mechanism links lymph- and angiogenesis

Shintaro Nakao, Souska Zandi, Yasuaki Hata, Shuhei Kawahara, Ryoichi Arita, Alexander Schering, Dawei Sun, Mark I. Melhorn, Yasuhiro Ito, Nuria Lara-Castillo, Tatsuro Ishibashi and Ali Hafezi-Moghadam

Blood (print ISSN 0006-4971, online ISSN 1528-0020), is published weekly by the American Society of Hematology, 2021 L St, NW, Suite 900, Washington DC 20036.